

This paper reports the advanced experimental-analytical method for determining the dynamic model of resonant converters of electricity. The object of research is semiconductor resonance converters and methods for analyzing their dynamics. The well-known experimental-analytical method for determining a dynamic model implements the sequence «experiment – analytics – dynamic model» when the structure of the system may be unknown. Then it is necessary to determine the structures and parameters of many dynamic models, among which the optimal ones will be selected. This makes it difficult to establish usable patterns.

Therefore, it is advisable to develop this method, according to which it is proposed to determine the parameters of the dynamic model according to the following sequence. First, carry out the analysis of the converter circuit and construct the dynamic models of sub-circuits. Next, an experiment is conducted with a simulation structural model of the converter, which is an input model of identification. After that, procedures are carried out for identifying and selecting optimal dynamic models among a set of initial identification models, as a result of which equivalent dynamics equations, gear ratios, and transfer functions of the selected converter models are obtained.

In the proposed modification of the method, the converter model is determined in advance, and at the identification stage it is enough to determine only its parameters. More simply, patterns are identified, and the number of initial identification models is significantly reduced. The results of using the proposed method on the example of determining the dynamic model of the charging resonance converter with inductive coupling between the charger and the battery of an autonomous object are given. The results of the presented analysis can be used in the design of resonant contactless chargers

Keywords: resonant charger, non-contact energy transfer, structural model, dynamic model

DETERMINING THE DYNAMIC MODEL OF THE CHARGING RESONANT CONVERTER WITH INDUCTIVE COUPLING BY AN EXPERIMENTAL-ANALYTICAL METHOD

Gennadiy Pavlov

Doctor of Technical Sciences, Professor
Department of Computerized Control Systems*

Andrey Obrubov

Corresponding author
PhD, Associate Professor
Department of Ship Power Systems*
E-mail: andrii.obrubov@nuos.edu.ua

Irina Vinnichenko

PhD, Associate Professor
Department of Computerized Control Systems*
*Admiral Makarov National University of Shipbuilding
Heroiv Ukrainy ave., 9, Mykolaiv, Ukraine, 54007

Received date 20.06.2022

Accepted date 17.08.2022

Published date 29.08.2022

How to Cite: Pavlov, G., Obrubov, A., Vinnichenko, I. (2022). Determining the dynamic model of the charging resonant converter with inductive coupling by an experimental-analytical method. *Eastern-European Journal of Enterprise Technologies*, 4 (8 (118)), 17–28. doi: <https://doi.org/10.15587/1729-4061.2022.263526>

1. Introduction

Semiconductor resonance converters have become quite popular in applications that require high energy efficiency, electromagnetic compatibility, and a decrease in the weight and size parameters of the finished integrated device. Recently, with the increase in demand for electric transport of mass and individual use, resonant inverters and converters based on them, which are capable of contactless transmission of electricity, require special attention. In particular, in order to achieve the competitive dynamic properties of the developed electric transport, it is first necessary to investigate the dynamics of the operation of semiconductor devices that underlie them, including resonant converters for contactless transmission of electricity.

The use of the experimental-analytical method for determining the dynamic model (DM) of the resonant converter is effective due to preliminary information on its scheme, according to which a structural model with causal relationships is built. The structural model replaces the real prototype converter in the experiment and corresponds to the converter's DM.

It is an input model that will be subject to parametric identification to determine relatively simpler equivalent DMs in the form of an output identification model (OIM). The validity of this method is based on the assumption that the simulation corresponds to real processes in the converter circuit. If the parameters of the model units that correspond to the sub-circuits of the converter are determined with sufficient accuracy, then the entire structural model of the converter will also correspond to its dynamic properties with sufficient accuracy. This approach makes it possible to circumvent the difficulties of a purely analytical way to build the DMs of converters of electricity with high-frequency switching of electrical circuits. Based on relatively simple linear models of subcircuits and nonlinear discrete links determined by analytical means, an equivalent compact in terms of DM expressions of a more complex converter system is created in the form of transfer functions or OIM equations. Therefore, the improvement of the experimental-analytical method for determining the dynamic model of the charging resonance converter with inductive coupling is a relative task.

2. Literature review and problem statement

The properties of resonance circuits with one or more oscillatory circuits, to which a similar circuit of a charging resonant converter (CRC) belongs, are well known in radio engineering and are described mainly for stationary modes [1]. In [2], a charging resonant LLC device is described, the calculations of electromagnetic processes in which are carried out by the method of finite elements but the calculations of its initial characteristics are performed at a static moment of operation of the converter, when they are conditionally considered unchanged. That is, they do not consider the overall dynamic pattern. In [3, 4], the authors pay attention to electromagnetic processes but carry out calculations only of their static characteristics. In the conversion equipment, considerable attention is also paid to the dynamics of resonant converters [5]. Thus, the development of laws for effective control of power supply systems is based on knowledge of dynamic characteristics. However, if the transfer functions have an order equal to the number of reactive elements of the converter substitution circuit, this may complicate the synthesis of stable controllers of automatic systems. For example, for a CRC substitution scheme, the order for the transfer function will be at least six. Therefore, scientists in this field apply methods for studying the dynamics of converters, which make it possible to obtain equivalent dynamics equations and transfer functions of smaller orders.

A DM in [5], built by the method of discrete transformation of Laplace, connects the discrete values of processes between adjacent references. Such a model is well consistent with pulse converters with a constant switching period but for converters with frequency or phase control with variable periods, such a model will be approximate. Therefore, the determination of the dynamic characteristics of impulse (essentially discrete) converters is sometimes performed using the method of continuous structural models [6] and equivalent continuous circuits [7]. According to those methods, the type of equivalent continuous link is determined from the dynamics equations or equivalent circuits of the power unit are compiled. Methods [6, 7] are convenient for transfer functions of only small orders (1–3). In other cases, the analysis of resonance circuits is also performed similarly to radio engineering, using the method of analysis on envelope oscillations [8]. They determine the relationship between the transfer function of the resonant network and the frequency characteristics of the converter, which makes it possible to take into consideration the action of the inverter-modulator with a rectifier-demodulator and reduce the order of DM. To determine the characteristics of resonant transducers near resonant frequencies, the method of the first harmonic is widely used [9, 10]. However, at a variable resonant frequency, as can be the case in a CRC with contactless energy transfer, this method may not give a sufficiently accurate result. A convenient approach to take into consideration some features of pulse converters that complicate determining equivalent DMs, such as switching circles with uncertain conditions, the nonlinearity of transfer characteristics, and impermanence of parameters, is experimental-analytical methods with system identification. These methods are relatively universal and suitable for the analysis of converters both according to a known structure – according to their schematic models [11, 12], and with an unknown structure – in the form of systems such as «black box» [13, 14]. However, the obtained OIMs only in sufficient quantities make

it possible statistically to establish patterns between the parameters of the schemes and their dynamic characteristics. Knowledge of these patterns is necessary to compensate for the parametric perturbations of power supply systems. On the other hand, the necessary patterns of processes are contained in the analytical DM but it can be too difficult to use in the synthesis of controllers.

The problem is that analytical and experimental methods for determining dynamic models of converters (as objects and systems with inputs and outputs in general) have characteristic disadvantages. By combining these methods, it is possible to reduce their shortcomings. As noted above, analytical methods can be difficult to use, yielding cumbersome mathematical expressions or systems of equations that will require simplifications and the introduction of a number of assumptions that will reduce their validity. Experimental methods give, so to speak, too individual results and, to obtain generalized patterns, require a large number of experiments with subsequent data processing. To circumvent the complexities of analytical methods and reduce the complexity of traditional experimental and analytical methods, it is advisable to combine the preliminary analytical definition of dynamic models of individual blocks of converters with the subsequent identification of their structural models as a whole.

Thus, in order to take advantage of analytical and experimental methods, it is advisable to supplement the experimental-analytical identification method with structural modeling of converters. The advantage of the structural model over the circuit model lies in the possibility of modeling the processes of converters with non-stationary parameters. The structural model is described by the dynamics equations and is essentially a graphic form of DM. This makes it possible to establish the desired patterns between the parameters of the circuit and the transfer functions. Machine modeling technology makes it easy to build a mixed structural model of CRC based on linear models of sub-circuits with permanent structures and based on nonlinear and discrete model blocks. In comparison, for example, with the structural-parametric identification of a circuit model or a prototype converter, automated parametric identification of the structural model [15] has the following advantages:

- the structural model in comparison with the schematic model is more visual from the point of view of the study of dynamics since it corresponds to the causal relationships between the links-sub-circuits;
- to build a structural model, it is enough to define analytical DMs only for linear subsets with a continuous structure, which is a simple task. As a result of identification, the DM scheme of CRC is determined by taking into consideration nonlinear and discrete elements;
- a smaller number of OIMs is subject to comparative analysis and the obtained OIMs may have a smaller order than a purely analytical DM of CRC.

3. The aim and objectives of the study

The aim of this study is to determine the dynamic model of the resonant converter, which will make it possible to obtain its dynamic characteristics. This will make it possible to investigate the dynamics of resonant converters by a modified experimental-analytical method even before the construction of experimental samples by building a structural

model of the converter as an object of identification. During the study, the following tasks were solved:

- to build a structural model of CRC;
- to determine the dynamic characteristics experimentally;
- to determine the equivalent transfer functions of CRC by methods of system identification.

4. The study materials and methods

4. 1. Object and hypothesis of research

The object of our research is semiconductor resonant converters of electricity and methods for analyzing their dynamics. As the investigated resonant converter, a charging resonant converter with the contactless transmission of electricity was considered.

The research hypothesis assumed the following. If the processes in the structural model of the resonant converter coincide with sufficient accuracy at the characteristic points of the set of working cycles with the processes of the experimental sample of the resonant converter, then the dynamic characteristics of the structural model will correspond with sufficient accuracy to the dynamic characteristics of the experimental converter.

The experimental-analytical method implements the sequence «experiment with a full-scale sample – analytics – dynamic model» when the structure of the system may be unknown. In this case, it is necessary to determine the structures and parameters of many dynamic models, among which the optimal ones will be selected. This makes it difficult to establish useful patterns. The development of this method lies in the fact that the analysis of linear sub-circuits of the converter with permanent structures is performed, their dynamic models are determined in the form of links with transfer functions. Then a converter model is composed of links, which also contain nonlinear links with interchangeable structures – an inverter and a rectifier. The parameters of the dynamic model are determined according to the sequence: «analytics 1 – experiment with model 1 – analytics 2 – model 2». Analytics 1 is the analysis of the converter circuit and the construction of dynamic models of sub-circuits. Model 1 – simulation structural model of the converter, which is the input model of identification. Analytics 2 are procedures for identifying and selecting optimal dynamic models among a set of initial identification models. Dynamic model 2 – equivalent dynamics equations, gear ratios, and transfer functions of the selected converter models.

4. 2. This study's scheme

The experimental scheme of CRC with non-contact energy transfer in Fig. 1 consists of inverter I, rectifier B, phase-shifting filter FZF, generator G. The resonance network (RM) consists of inductors L_1 (transmitting) and L_2 (receiving), capacitors C_1 and C_2 to compensate for parasitic inductances. The input of the CRC power supply is connected to the voltage of the energy source $u_s = U_{s0} + \Delta u_s$ with constant U_{s0} and variable Δu_s components, which represents the rectified voltage of the power network or another source of unstable voltage (generators, solar cells, batteries, etc.). The output of CRC is connected to the consumer of energy – a source of constant voltage U_q , which is represented by a rechargeable battery that receives electricity and is charged. In charging mode, coils close to each other have a mutual inductance M . Magnetic connection coefficient between coils is

a parametric input value and can vary widely in the process of modeling $k_m = 0 \dots 1$. The inverter operates under two modes. The first is the forced generation mode with a constant frequency F_g . At the same time, the PSK control signal switch is in the left position «P» and the inverter receives a control signal from the generator. The second mode is the self-generation mode, in which the inverter control voltage is induced from the signal of the current sensor i_1 of the primary circuit. This signal passes through ZF and is fed to control the inverter. Then PSC is in the right position «A».

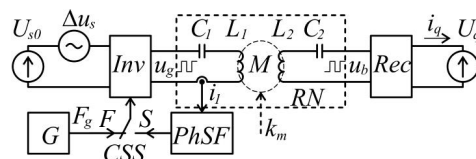


Fig. 1. Scheme for studying the dynamics of the charging resonance converter: *Inv* – inverter, *Rec* – rectifier, *RN* – resonant network, *G* – generator, *CSS* – control signal switch with positions of forced generation *F* and self-generation *S*, *PhSF* – phase-shift filter

The DM of CRC is determined in three stages. Firstly, based on theoretical analysis of the CRC circuit, its computer structural model is built, which consists of linear transfer links of proportional or integral types and nonlinear discrete links. Secondly, experimentally, using the structural model of the CRC, some of its static and dynamic characteristics are determined. Among them are the gear ratio, transient characteristics of the output current, the dependence of the output current on the magnetic coupling coefficient between the coils $I_q(k_m)|_{U_q=\text{const}}$; the dependences of the operating frequency of self-generation on the magnetic coupling coefficient between the coils $F_g(k_m)|_{U_g=\text{const}}$. The transfer characteristic is the dependence of the output current on the supply voltage at a constant output voltage $I_q(U_s)|_{U_q=\text{const}}$. The transient characteristics of the output current are determined in continuous $i_q(t)|_{U_q=\text{const}}$ and discrete $i_q(n)|_{U_q=\text{const}}$ time. Thirdly, these experimental data are automatically normalized, analyzed by regression analysis methods and, as a result, the OIM transfer functions are found, close in dynamic characteristics to the CRC under a certain mode of operation.

4. 3. Parameters of the structural model and methods of analysis of experiment data

The experimental part of our research was carried out in the MATLAB package using the Simulink simulation system and the Ident GUI application from the System Identification Toolbox. The structural model of CRC is implemented as a Simulink model in Fig. 2, *a* according to the diagrams in Fig. 4, 5, 7–10. When simulating the processes of the CRC, the following simulation options were set: Stop Time=200, 500, 1000 (selected for different conditions); Solver Options: Variable Step, Max step size=0.001. In the model, we use the method of calculating ode15s (stiff/NDF), which calculates the state of the model using numerical variable-order differentiation formulas (NDF), which are associated with the Gere method but more efficient [15]. Other simulation options are set by default.

Next are the parameters of the structural model of the CRC. The rated supply voltage $U_{s0} = 1$ V. Output voltage $U_q = 0.5$ V. Frequency of inverter generator $F_g = 1$ Hz. The parameters of the elements of the RM were chosen to be

the same for the primary and secondary sides since the transmitting and receiving coils can also be the same. Therefore, the transformation coefficient $n=1$. The inductance of the coils $L_{1,2}=1.27$ Gn. The capacitance of capacitors $C_{1,2}=2$ F. Serial equivalent loss resistance $r_{1,2}=0.0159$ Ohm. Quality of each serial RLC-chain $Q_{1,2}\approx 5$. With a magnetic coupling coefficient $k_m=0.99$, the scattering inductance, according to (5), is $L_{s1}=L_{s2}=0.0127$ Gn, and the resonance frequency of the series RLC circuit is $f_0\approx 1$ Hz, the free oscillation frequency is $f_1\approx 0.994$ Hz (respectively, the angular frequencies $\omega_0=2\pi f_0$, $\omega_1=2\pi f_1$). Wave impedance $\rho_{1,2}=0.08$ Ohm. The real values of the magnetic coupling coefficient for charging systems of vehicles where the inductors are at certain distances from each other, are in the range of $k_m=0.7-0.85$ [16]. For charging systems with magnetic connectors, the values are significantly higher and can reach $k_m=0.95-0.995$. The RM parameters can be scaled for new values of the supply voltage $L'_{1,2}=U'_{s0}L_{1,2}$, $C'_{1,2}=C_{1,2}/U'_{s0}$, $r'_{1,2}=U'_{s0}r_{1,2}$, of the operating frequency $L'_{1,2}=L_{1,2}/f'_g$, $C'_{1,2}=C_{1,2}/f'_g$, of the rated output current $L'_{1,2}=L_{1,2}/k_I$, $C'_{1,2}=k_I C_{1,2}$, $r'_{1,2}=r_{1,2}/k_I$. Here, k_I is the coefficient of change in the rated output current.

In the course of model experiments, the supply voltage was changed by several degrees. Removal of transient characteristics of the output current $i_q(t)$ in continuous time and current I_{qm} in discrete time was performed after the structural model of the CRC reached the rated mode on the second step of the supply voltage. This is due to the fact that the CRC manifests itself as a significantly nonlinear transmission link in the start-up area for small input values (0–30 % of rated). The input of the structural model of the CRC was initially supplied with a rated voltage U_{s0} and after entering the rated mode and the end of the transients, the following degree of supply voltage Δu_s was added, which was 10 % of the rated voltage (first stage). The simulation lasted at least until the damping of the free components and the establishment of a steady-state mode of operation. To fix the average value of the output current in each half-period of the inverter oscillations at the output of the structural model, the current average fixator in Fig. 2, b. inverter at the output of the structural model we used a clamp of the current average in Fig. 2, b. It integrates every n th half-wave of current $i_q(t)_n$ and divides its integral by the measured half-wave period T_n . At the output, the next average value I_{qn} is fixed.

The simulation results of transients were stored in the MATLAB working area as an array of input and output values $yout$, and an array of simulation time $tout$. Then they were processed using a program in an m -file. Processes from the beginning of the second stage of the supply voltage were separated, brought to the beginning of coordinates, and to a unit value. Further, they were uniformly thinned with the step T_{cp} (average period of current half-waves during the simulation time). Along the way, the current gain of the CRC $K_{UI}=\Sigma\Delta I_{qn}/\Sigma\Delta u_{sn}$ was calculated for data areas when the values of the output current I_{qn} reached a constant value. For the identification procedure, the $Ainput$ and $Aoutput$ arrays were formed as a result of the experiment with the data of normalized transient processes. The discreteness step of the normalized data was taken as unity and with single constant values of increments of quantities.

The identification of the structural model of the CRC as a linearized discrete system was performed in the Ident GUI application from the System Identification Toolbox section. $Ainput$ and $Aoutput$ arrays obtained from simulation data were imported as derived data. The discreteness step was

set to $Samp. interv.=1$. In the process of identification at the output of each procedure $Estimate\rightarrow Parametric models$ we automatically built so-called arx -models of certain orders and a certain system delay ($N_p=2...4$, $N_z=1...4$, $\tau=0...3T$), which were set manually in advance. Such OIMs were chosen that would ensure the slightest deviations of their own processes from the processes at the output of the structural model of the CRC.

A variation of types of OIM in MATLAB is the polynomial mathematical arx model (*Autoregressive with Extra Input*), which is the equation of a discrete-continuous system:

$$A(q)y(t)=B(q)u(t-\tau)+e(t),$$

where $A(q)=1+a_1q^{-1}+a_2q^{-2}+...+a_Nq^{-N_p}$, $y(t)$ is the initial value of the system, $B(q)=b_0+b_1q^{-1}+b_2q^{-2}+...+b_Mq^{-N_z}$, $u(t)$ is the input value of the system; here, it is also indicated: N_p – the number of poles, N_z – the number of zeros of the transfer function, q – delay operator: $q^{-1}u(t)=u(t-T)$, τ – the input delay of the system. A discrete-continuous system has discrete time delays multiple to a fixed period T , and continuous input and output values. If in this system the input value $u(t)$ is also discrete $u(nT)$, then the system can be represented as completely discrete. Then the above equation can be rewritten in operator form, where q replaces the operator $z=e^{pT}$ and instead of discrete functions of time, the equations contain their operator representations ($u(nT)\rightarrow u(z)$).

Deviations between the processes in the OIM and in the structural model of the CRC were evaluated according to two criteria. The value of the first criterion – standard error (LF – Loss function) is:

$$LF = \sum_{j=1}^N w_j (f(x_j) - y_j)^2,$$

where j is the number of data elements, N is the number of elements in the data set, x_j is the input values of the system, y_j is the output values of the system, $f(x_j)$ is the projected output values of the OIM, w_j is the weight coefficients, the sum of which is equal to unity.

The second criterion is the final prediction criterion by Akaike (FPE – Final Prediction Error), which evaluates the quality of OIM when the structural model is tested on a different dataset. After calculating several different OIMs, one can compare them according to this criterion. According to Akaike's theory, the most accurate OIM has the smallest FPE . The final prediction error of Akaike (FPE) is determined from the following equation:

$$FPE = LF(1 + d / N) / (1 - d / N),$$

where LF is the criterion of standard error, d is the number of parameters evaluated, N is the amount of data.

Discrete-continuous transfer functions of OIM with a period $T=1$ can also be applied to other values of the discreteness period. To bring the DM to the real scheme of CRC in time, it is sufficient to go to a discreteness period equal to the half-wave period of the rectified current $T=1/2fg$ instead of a single discreteness period. In this case, the coefficients of the transfer function will not change if the inductances and capacitances of the power circuit of CRC during the transition to another time scale change inversely proportional to the change in the rated operating frequency.

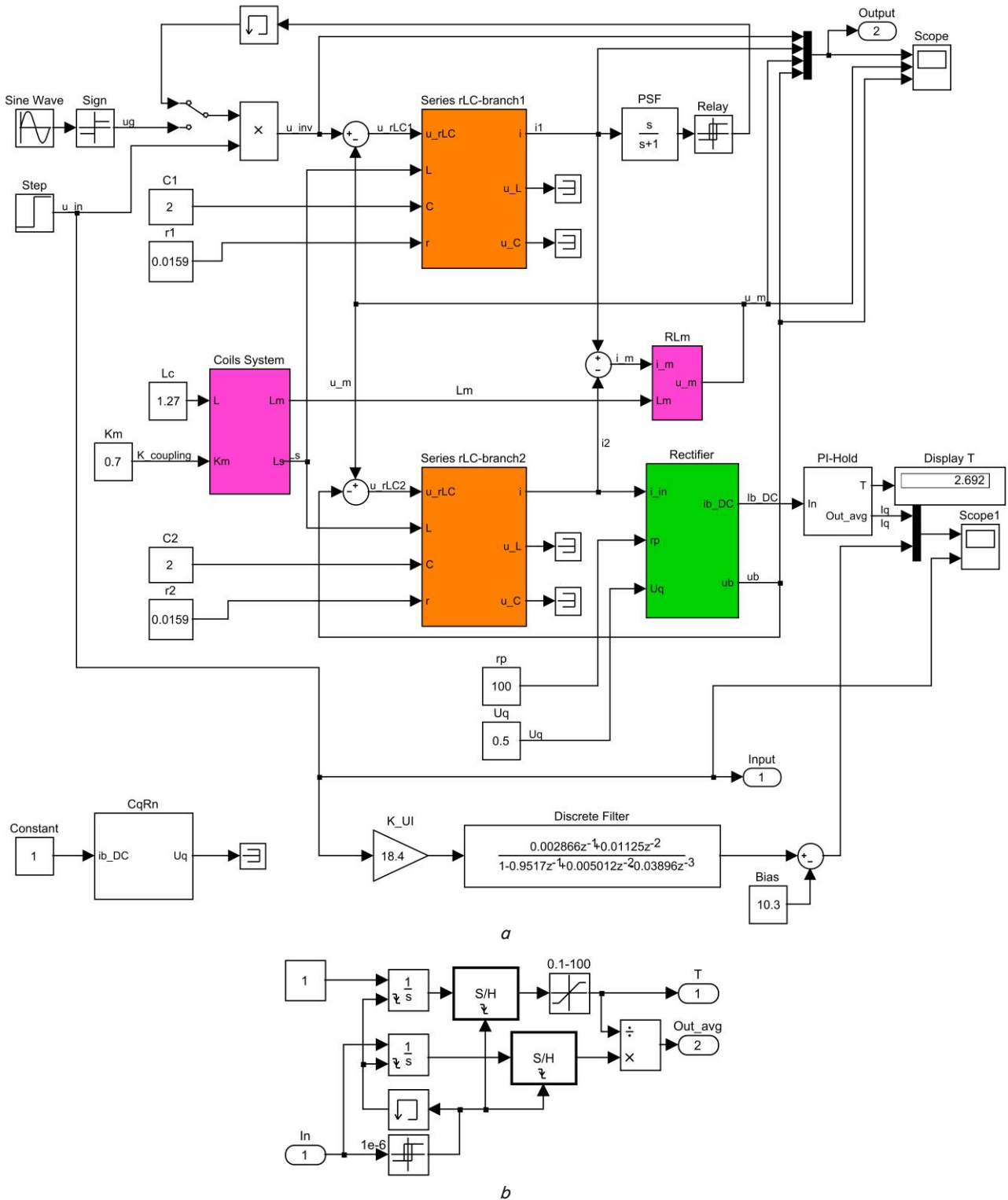


Fig. 2. Simulink-model scheme: *a* – charging resonance converter; *b* – retainer of the current average value *Pi-Hold*

5. Results of studying the charging resonance converter

5.1. Structural model of the converter

The structural model of CRC is explained by the T-shaped scheme of substitution of RM in Fig. 3 with sources of alternating voltages at the input and output of the circuit: u_g – the output voltage of the inverter and u_b – the input voltage of

the rectifier. Conductivities Y_1 and Y_2 contain active resistances, inductances, and capacitances. Resistance Z_m consists of active resistances and inductance.

According to the scheme in Fig. 3, we have the equation of voltages at conductivities Y_1 and Y_2 , and current through resistance Z_m :

$$u_{Y1} = u_g - u_m \text{ and } u_{Y2} = u_m - u_b, \quad i_m = i_1 - i_2, \quad (1)$$

which corresponds to the block diagram of the block model of the CRC in Fig. 4. The input values of the structural model of the CRC are the supply voltage u_s and the output voltage U_q . The main output value is the output current (consumer current) i_q . There are additional outputs for controlling the processes of the circuit – currents i_1 and i_2 of the primary and secondary circuits.

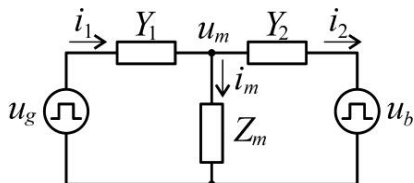


Fig. 3. T-shaped resonant network substitution circuit: u_g – inverter output voltage, u_b – rectifier input voltage

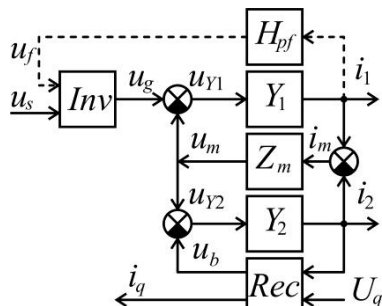


Fig. 4. Block diagram of the structural model of the charging resonance converter: *Inv* – inverter, *Rec* – rectifier

Briefly, the principle of operation of the structural model of CRC can be described as follows. In inverter I, a rectangular voltage u_g is generated, the amplitude of which is set by the value of the supply voltage u_s . The frequency of the output voltage can be constant F_g or variable f_{ag} and determined by the signal u_f of positive feedback on the current of the primary circuit. Due to the feedback action, the frequency of the inverter f_{ag} automatically adjusts close to the resonant frequency f_{01} of the primary circuit i_1 , which contributes to better compensation for the parasitic inductances of the scattering of the coils. Under the action of voltage u_g , a current i_1 passes in the primary circuit, which is divided into the current of the secondary circuit i_2 and the magnetization current i_m . The current of the secondary circuit i_2 is rectified and enters the consumer (battery) in the form of current i_q . The output voltage U_q is applied to the other input, which also affects the magnitude of the output current i_q . The structural model in Fig. 4 makes it possible to investigate the dynamics of CRC by the input of the supply voltage u_s , the output voltage U_q , the frequency f_g and by parametric inputs. Output values are the currents of the circuits i_1 and i_2 and the output current i_q . It is also possible to investigate the self-generation frequency f_{ag} .

5. 2. Determining dynamic characteristics

5. 2. 1. Structural models of converter sub-circuits

Blocks in the structural model in Fig. 4 correspond to the sub-circuits of the electrical circuit of the converter. These blocks as transmission links are divided by input and output signals (current or voltage) into *ii-links*, *iu-links* (operator supports Z), *ui-links* (operator conductivities Y), and *uu-links*. Block structures, in turn, consist of inertial and inertial transmission links. Reactive elements are modeled

only by integral links. This ensures compliance with the laws of switching when the inductance current or voltage on the capacitance cannot be replaced instantly or by a step function. Let us consider in detail the structural models of the sub-circuits – first, the elements RM Y_1 , Y_2 , and Z_m for the CRC in Fig. 1.

The total conductivities Y_1 and Y_2 are sequential resonant RLC circuits consisting of sequentially activated inductance L, capacitance C, and active resistance r_s in Fig. 5, a. At $r_s < 2\sqrt{L/C}$ (the quality of the circuit will be $Q > 0.5$) free processes in RLC-circuit will be oscillatory in nature and at periodic external voltage u with frequencies close to $f_0 = 1/(2\pi\sqrt{LC})$ the result will be a resonance effect, which is often used in electricity converters [2, 5, 7–9]. Therefore, these RLC-circuits are called resonant. First, we take as an input value the total voltage u on the RLC circuit, and for the output value – its current i_r . That is, we represent the resonant circuit as conductivity Y (*ui-link*).

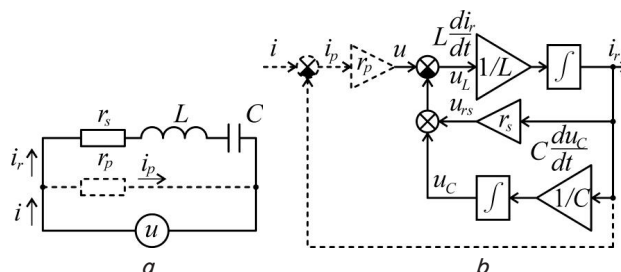


Fig. 5. Sequential resonant circuit: a – circuit; b – structural model (the dotted line shows an additional part for conversion to *ii(iu)*-link)

The differential equations of the processes of the scheme in Fig. 4 will take the form:

$$\begin{cases} L \cdot di_r/dt = u - i_r r_s - u_c; \\ C \cdot du_c/dt = i_r, \end{cases} \tag{2}$$

where u_c is the voltage on the capacitance. Equation (2) corresponds to the structural model in Fig. 5, b, which is already a *ui(uu)*-link with one input u and two outputs i_r and u_c .

To determine the transfer function, we rewrite (2) in matrix form:

$$\frac{d}{dt} \begin{bmatrix} i_r \\ u_c \end{bmatrix} = \mathbf{A} \cdot \begin{bmatrix} i_r \\ u_c \end{bmatrix} + \mathbf{B} \cdot u, \tag{3}$$

where

$$\mathbf{A} = \begin{bmatrix} -r_s/L & -1/L \\ 1/C & 0 \end{bmatrix}$$

is the system matrix,

$$\mathbf{A} = \begin{bmatrix} -r_s/L & -1/L \\ 1/C & 0 \end{bmatrix}, \mathbf{B} = \begin{bmatrix} 1/L \\ 0 \end{bmatrix}$$

is the input matrix.

Then the matrix transfer function takes the form:

$$\begin{aligned} \mathbf{H}(s) &= \begin{bmatrix} i_r \\ u_c \end{bmatrix} \cdot u^{-1} = \mathbf{O} \cdot (s \cdot \mathbf{I} - \mathbf{A})^{-1} \cdot \mathbf{B} = \\ &= \begin{bmatrix} sC / (s^2 LC + sCr + 1) \\ 1 / (s^2 LC + sCr + 1) \end{bmatrix} = \begin{bmatrix} sC / ((s/\omega_0)^2 + s/Q\omega_0 + 1) \\ 1 / ((s/\omega_0)^2 + s/Q\omega_0 + 1) \end{bmatrix}, \end{aligned} \tag{4}$$

where u is the input value,

$$Y(s) = \mathbf{H}_1(s) = sC / \left((s/\omega_0)^2 + s/Q\omega_0 + 1 \right)$$

is the conductivity of the RLC circuit, s is the Laplace operator. Contour parameters: $Q = \rho/r$ – quality, $\omega_0 = 1/\sqrt{LC}$ – resonance frequency, $\rho = \sqrt{L/C}$ – wave impedance.

To convert the subcircuit to the $ii(iu)$ -link, where the input value instead of the voltage source u will be the current i , one can enter an additional parallel resistance r_p , as shown by the dotted line in Fig. 5. The voltage on the RLC circuit will be expressed through an additional parallel resistance $u = (i - i_r)r_p$. This will make it possible not to change the original mathematical model of the subcircuit (2) and the structural model in Fig. 5, b , adding to it the elements shown by the dotted line. The value of the additional parallel resistance should be chosen relatively large $r_p \gg \sqrt{L/C}$ or $r_p \gg r_s$ so that its influence on the processes in the circuit is negligibly small.

The channel for non-contact energy transmission from source u_s to consumer with voltage $u_c U_q$ in Fig. 1 are two closely spaced coils with a significant magnetic coupling between them in Fig. 6, a . The coil system is characterized by inductances L_1 and L_2 , active resistances r_1 and r_2 , mutual inductance $M = k_m \sqrt{L_1 L_2}$ and magnetic coupling coefficient, which can slowly change within $k_m = 0 \dots 1$. Parallel resistances r_{d1} and r_{d2} (shown by the dotted line) simulate active losses due to eddy currents. We shall consider the voltage u_1 and the current i_1 as input values, and the voltage u_2 and the current i_2 as the output values.

Some assumptions have been made that do not fundamentally affect the achievement of the objectives of this study: with changes in the relative position of the coils, only the mutual inductance M changes without changing the inductances of the coils L_1 and L_2 . This is possible when there are no ferromagnetic elements in the system and the change in the relative position of the coils does not change the magnetic resistance for its own fluxes. Also, suppose that the same magnetic flux passes through each turn of a separate coil (the coils are thin rings). As a result, when the magnetic coupling coefficient between the coils $k_m = \text{var}$ changes, the transformation coefficient will be unchanged $n = \text{const}$, which makes it possible to consider this coil system

as a linearized transformer in Fig. 6, b with the following parameters:

– transformation coefficient $n = \sqrt{L_1/L_2} = \omega_1/\omega_2$, where L_1 and L_2 – complete primary and secondary inductances, ω_1 and ω_2 – the number of turns of the primary and secondary coils;

– magnetic coupling coefficient $k_m = M/\sqrt{L_1 L_2}$, where M is mutual inductance.

The inductances of the primary and secondary windings of the transformer are divided into two parts $L_1 = L_{s1} + L_{m1}$ and $L_2 = L_{s2} + L_{m2}$, which are described by the following ratios:

$$L_{s1} = L_1(1 - k_m), \quad L_{s2} = L_2(1 - k_m),$$

$$L_{m1} = L_1 k_m, \quad L_{m2} = L_2 k_m, \quad (5)$$

where L_{s1}, L_{s2} – scattering inductors whose magnetic fluxes are separate, L_{m1}, L_{m2} – fully connected to each other inductors that have a common magnetic flux. Equivalent resistances of active losses are also divided into two parts $r_1 = r_{ds1} + r_{dm1}$ and $r_2 = r_{ds2} + r_{dm2}$, which may have different reciprocal relationships than parts of inductances in (5).

The processes in each of the two similar RL circuits in Fig. 6, a at zero currents in the other circuit can be described by the equations:

$$u_L = L \frac{d}{dt} (i - u_L/r_d), \quad u_L = r_d \left(i - \frac{1}{L} \int_0^t u_L dt + i_L(0) \right),$$

$$i = \frac{1}{r} (u_{RL} - u_L), \quad (6)$$

where u_L is the voltage at the inductance L, r_d – parallel resistance, i – total circuit current, r – serial resistance, u_{RL} – total circuit voltage.

Equation (6) corresponds to the structural model in Fig. 7, a , which we take as the basis of the structural model of the circuit in Fig. 6, b and the T-shaped transformer substitution scheme in Fig. 6, c with the given parameters of the primary side to the secondary side: $L_1^* = L_1/n^2$; $r_1^* = r_1/n^2$; $i_1^* = n \cdot i_1$; $u_1^* = u_1/n$, where the reduced values $L_{s1}^*, L_{m1}^*, r_{d1}^*, i_{m1}^*, u_{m1}^*$ will also be determined in a similar way.

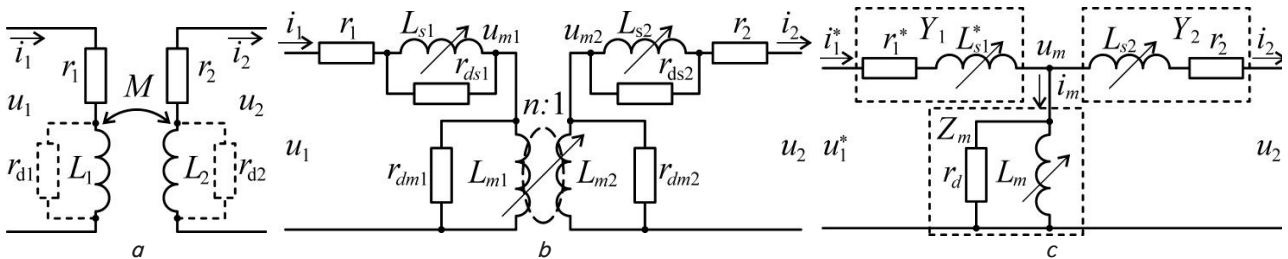


Fig. 6. Schemes: a – magnetically connected coils with mutual inductance M ; b – linearized transformer with separated windings; c – T-shaped substitution scheme with given primary parameters

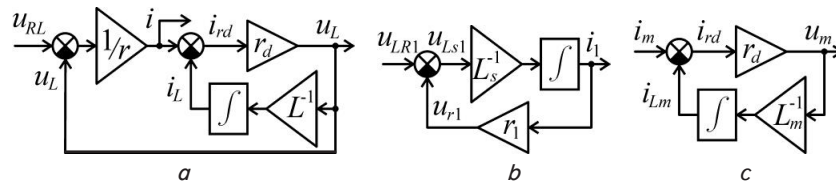


Fig. 7. Structural models of RL circuits: a – with serial r and parallel r_d resistances and with the transfer function $H_{RL}(s)$; b – only with sequential active resistance ($r_d = \infty$) and with full conductivity $Y_1(s)$; c – only with parallel active resistance ($r = 0$) and with full resistance $Z_m(s)$

The ratios of inductances for the T-shaped transformer replacement circuit will be [17]:

$$L_{s1} = L_1(1 - k_m/n), L_{s2} = L_2(1 - k_m/n),$$

$$L_m = L_1 k_m/n = L_2 k_m/n. \tag{7}$$

In the diagram in Fig. 6, c, expressions (7) become similar to expressions (5), which will exclude negative inductance values undesirable in structural models at certain values of n .

Usually, with coils close to each other, the most significant losses of magnetization occur in a common field of coils. Therefore, in the T-shaped substitution scheme at values of k_m close to one, resistances r_{ds1} and r_{ds2} can be ignored. They can be taken close to infinity, and losses on eddy currents can be considered concentrated in a single parallel resistance $r_d = r_{dm1}^* \cdot r_{dm2}^* / (r_{dm1}^* + r_{dm2}^*)$, where $r_{dm1}^* = r_{dm1}/n^2$ – the reduced primary resistance to magnetization losses. Then the structural model in Fig. 7, a will be replaced by structural models of the serial chain $r_1 L_1$ (or $r_2 L_2$) in Fig. 7, b, and parallel chain $r_d L_m$ in Fig. 7, c. The transfer functions of their structural models will accordingly take the form:

$$H_{RL}(s) = \frac{\rho L/r}{sL(r+r_d)/(r \cdot r_d) + 1},$$

$$Y_1(s) = \frac{1/r_1}{sL_1/r_1 + 1}, Z_m(s) = \frac{sL_m}{sL_m/r_d + 1}, \tag{8}$$

where the expression $Y_2(p)$ will be similar to the expression $Y_1(p)$.

Substitution scheme in Fig. 6, c is similar to the RM substitution scheme in Fig. 3. Therefore, according to (1), using the structural models of *RL-chains* in Fig. 7, b, c, it is possible to build a structural model in Fig. 8, a for the diagram in Fig. 6, c. Dashed lines show the parametric effects $L_{s1}^* = L_{s2} = L_2(1 - k_m)$, $L_m = L_2 k_m$ at $k_m = 0 \dots 1$. The generalized flowchart of this structural model in Fig. 8, b is consistent with the diagram in Fig. 4.

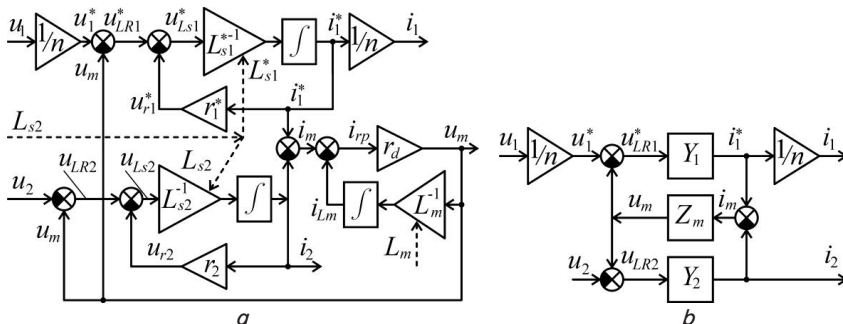


Fig. 8. Structural models: a – T-shaped transformer substitution circuit with variable magnetic coupling coefficient; b – resonant network (generalized flowchart)

The processes of both structural models can be described by equations of the following type in operator form (for the scheme in Fig. 4 at $n=1$):

$$i_1(s)n = (u_1(s)/n - u_m(s))Y_1(s),$$

$$i_2(s) = (u_m(s) - u_2(s))Y_2(s),$$

$$u_m(s) = (i_1(s)n - i_2(s))Z_m(s), \tag{9}$$

or in matrix form $\mathbf{x} = \mathbf{A} \cdot \mathbf{x} + \mathbf{B} \cdot \mathbf{u}$, where

$$\mathbf{x} = \begin{bmatrix} i_1(s) \\ i_2(s) \end{bmatrix}, \mathbf{u} = \begin{bmatrix} u_1(s) \\ u_2(s) \end{bmatrix},$$

$$\mathbf{A} = \begin{bmatrix} -Z_m(s) \cdot Y_1(s) & Z_m(s) \cdot Y_1(s)/n \\ Z_m(s) \cdot Y_2(s)n & -Z_m(s) \cdot Y_2(s) \end{bmatrix},$$

$$\mathbf{B} = \begin{bmatrix} Y_1(s)/n^2 & 0 \\ 0 & -Y_2(s) \end{bmatrix}.$$

The solution to (8) is the matrix transfer function of RM CRC:

$$\mathbf{H}(s) = \mathbf{x} \cdot \mathbf{u}^{-1} = (\mathbf{I} - \mathbf{A})^{-1} \cdot \mathbf{B} = \begin{bmatrix} H_{11}(s) & H_{12}(s) \\ H_{21}(s) & H_{22}(s) \end{bmatrix}, \tag{10}$$

where

$$H_{11}(s) = \frac{1}{n^2} \cdot \frac{Y_1(s) \cdot (1 + Z_m(s) \cdot Y_2(s))}{1 + Z_m(s) \cdot (Y_1(s) + Y_2(s))} = \frac{i_1(s)}{u_1(s)},$$

$$H_{12}(s) = -\frac{1}{n} \cdot \frac{Z_m(s) \cdot Y_1(s) \cdot Y_2(s)}{1 + Z_m(s) \cdot (Y_1(s) + Y_2(s))} = \frac{i_1(s)}{u_2(s)},$$

$$H_{21}(s) = \frac{1}{n} \cdot \frac{Z_m(s) \cdot Y_1(s) \cdot Y_2(s)}{1 + Z_m(s) \cdot (Y_1(s) + Y_2(s))} = \frac{i_2(s)}{u_1(s)},$$

$$H_{22}(s) = -\frac{Y_2(s) \cdot (1 + Z_m(s) \cdot Y_1(s))}{1 + Z_m(s) \cdot (Y_1(s) + Y_2(s))} = \frac{i_2(s)}{u_2(s)},$$

$u_1(s)$ and $u_2(s)$ are the input values, $i_1(s)$ and $i_2(s)$ – output values, s – Laplace operator. Expressions of operator conductivities Y_1 and Y_2 for a non-resonant circuit of a converter with a transformer are taken from (8) as the conductivity of the *RL* circuit, and for the CRC – from (4) as the conductivity of the *RLC* circuit. The expression of the magnetization resistance Z_m is taken from (8). Thus, the structural model of CRC is built based on the structural model of the RM in Fig. 8, b.

Next, consider the structural models of the inverter and rectifier. The inverter can be represented as an amplitude modulator of alternating rectangular voltage in Fig. 9, which is formally described by the following expression $u = u_s \Sigma \Pi(t - nT) (-1)^n$, where $u_s = U_{s0} + \Delta u_s$ with constant U_{s0} and variable Δu_s components, $n = 0, 1, 2, \dots$ – half-period number, $P(t) = 1(t) - 1(t - T)$ is the function of rectangular momentum length T , $1(t)$ – function of a unit rectangular power.

The input value of the inverter is the low-frequency variable component Δu_s , which simulates the instability of the supply voltage.

The output value is a rectangular voltage u_g , the amplitude of which is equal to the supply voltage u_s . Signal of the primary current i_1 and band FZF with a transfer function of the form:

$$H_{pf} = s\tau_{pf} / (1 + s\tau_{pf}),$$

is used to synchronize the inverter under a self-generation mode.

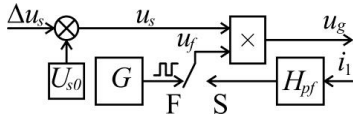


Fig. 9. Block diagram of inverter model: G – constant frequency pulse generator, H_{pf} – phase shift filter transmission function

At the input of the rectifier made of diodes $VD1-VD4$ in Fig. 10, a , the alternating current of the secondary circuit RM CRC i_2 is supplied, which is rectified and passes through the energy consumer u_q in the form of a rectified current $|i_b|$, where $i_b = i_2 - i_{rp}$. Resistance r_p at the rectifier input simulates losses on the leakage current i_{rp} from the rectifier input side at reverse voltages on the diodes. Structural model of the rectifier in Fig. 10, b consists of linear and nonlinear links and takes into consideration the voltage drop on the diodes in the forward direction $u_{VD} = 2U_{VD_for}$. Input values of the structural model of the rectifier are current i_2 and output voltage u_q . Output values are rectified current $|i_b|$ and input voltage u_b .

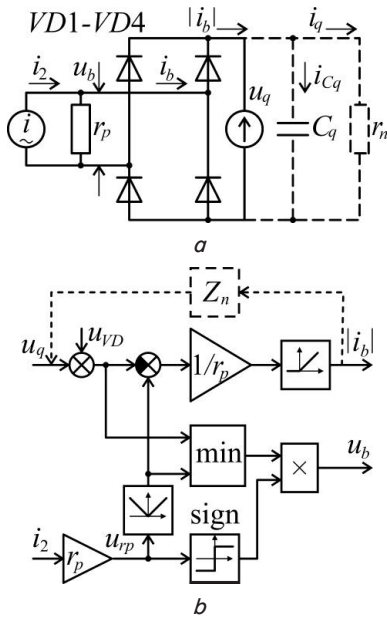


Fig. 10. Bridge rectifier: a – circuit; b – structural model

If it becomes necessary to investigate CRC with a different type of load than the rechargeable battery, for example, dotted line on the diagrams of Fig. 10 shows the connection of the resistive load r_n with the filtering capacity C_q instead of the consumer in the form of a voltage source u_q . Then the output voltage will be determined as $u_q = (|i_b| - u_q/r_n) / sC_q$, hence one can express the resistance of the load circuit $Z_n = u_q / |i_b| = r_n / (1 + sC_q r_n)$ for the structural model in Fig. 10, b .

5. 2. 2. Static characteristics

In the course of experimental studies of the structural model of the CRC, a number of static and dynamic characteristics were obtained. Below are some static characteristics, the data for which were taken from data areas where the processes acquired a stationary character and then were determined as average values from several experiments. Characteristics were acquired at a constant output voltage $U_q^* = 0.5$. The values of the voltages on the characteristics are indicated in units relative to rated values.

Fig. 11 shows the transfer characteristics of the CRC for power supply – the dependence of the output current on the supply voltage $I_q(U_s)_{U_q=\text{const}}$ in the operating range of the supply voltage at a constant output voltage.

Fig. 12 shows the dependence of the output current on the magnetic coupling coefficient between the coils $I_q(k_m)_{U_q=\text{const}}$ for forced generation (A) and self-generation modes (B, C) with different FZF time constants and supply voltage values (curves 1 and 2).

Fig. 13 shows the dependence of the operating frequency under the self-generation mode of CRC on the magnetic coupling coefficient between the coils $F_g(k_m)_{U_q=\text{const}}$ for different PhSF time constants.

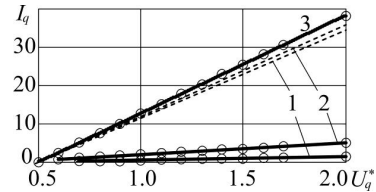


Fig. 11. Transfer characteristics $I_q(U_q)$: 1 – $k_m=0.95$; 2 – 0.97; 3 – 0.99 (solid lines – forced generation mode, dashed lines – self-generation mode)

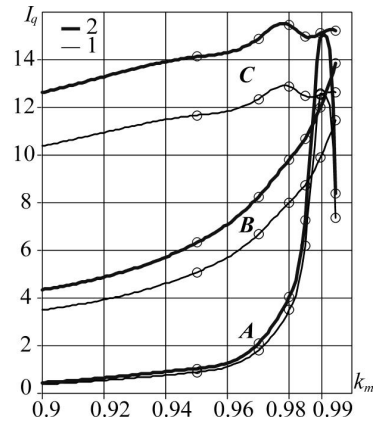


Fig. 12. Plots of the dependence of the output current on the magnetic coupling coefficient $I_q(k_m)$: A – for forced generation with a frequency $F_g=1$ Hz, B – for self-generation at $\tau_{pfr}=0.2$ s, C – for self-generation at $\tau_{pfr}=1.0$ s; 1 – $U_s^*=1$; 2 – $U_s^*=1.1$

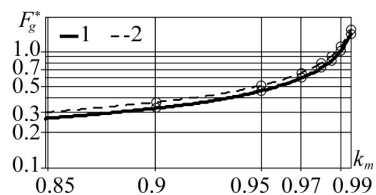


Fig. 13. Dependences of the self-generation frequency of the charging resonance device on the magnetic coupling coefficient: 1 – $\tau_{pfr}=1.0$ s; 2 – $\tau_{pfr}=0.2$ s

On the static characteristics, the rings marked the experimental points of the argument values, in which the average values of the values-functions were calculated according to the data of a series of experiments with the structural model of CRC.

5. 2. 3. Dynamic characteristics

Below in Fig. 14, we show plots of the processes of the structural model of the CRC when modeled in Simulink.

Fig. 15 shows the normalized transient characteristics of the structural model of CRC and the transfer functions of OIM, taken at $\Delta U_s^* = 0.1$, $U_q^* = 0.5$ for several values of the magnetic coupling coefficient k_m between the coils.

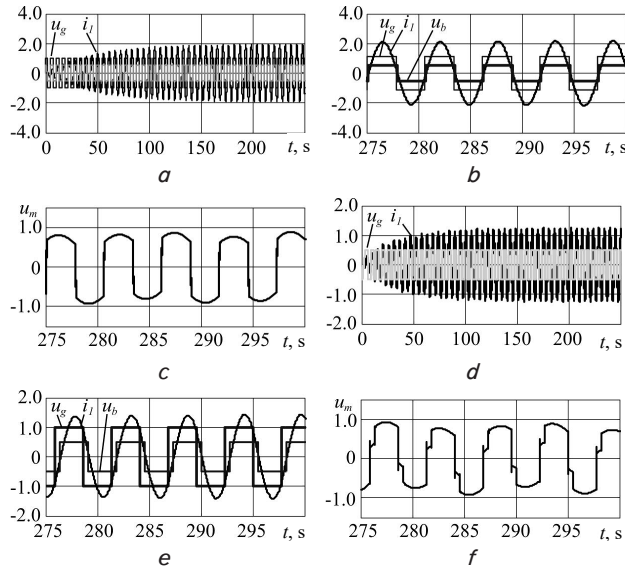


Fig. 14. Plots of processes in the resonant network of the structural model of the charging resonance device with $k_m=0.7$: *a–c* – for the forced generation mode; *d–f* – for self-generation mode; *a, b* – an increase in fluctuations at startup; *b, d* – voltages of the inverter u_g , rectifier u_b , and current of the primary circuit i_1 (current on a scale of 0. 1)

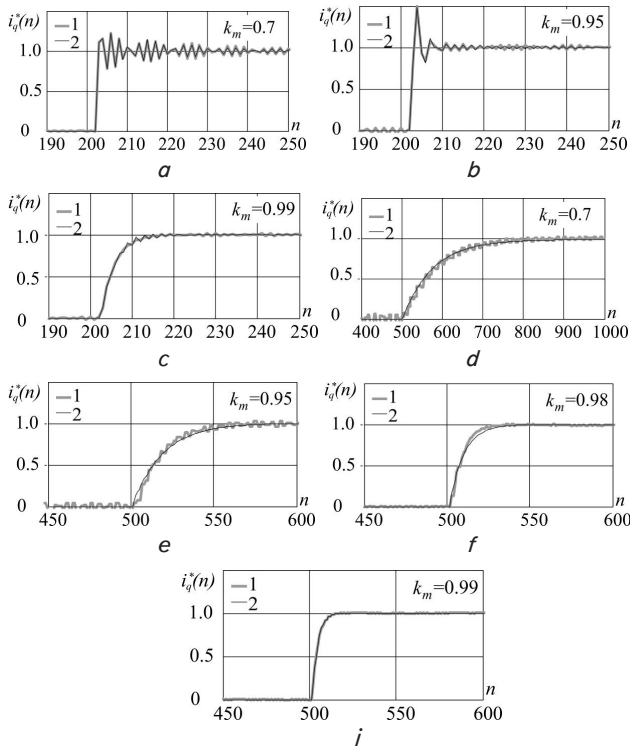


Fig. 15. Transient characteristics of the charging resonance device and the output identification model: *a–c* – for the forced generation mode; *d–j* – for self-generation mode, 1 – output signal of the structural model of the charging resonance device, 2 – output signal of the output identification model

From the plots of transient characteristics (Fig. 15) it can be seen that at lower values of the coupling coefficient k_m , the transients are oscillatory.

5. 3. Transfer functions

As a result of automated identification by the least squares method, the Ident GUI produced the following normalized transfer functions of OIM the type of *arx441* [15], magnetic coupling coefficients, and deviation criteria for the forced generation mode at $F_g=1$ Hz:

$$H(q) = \frac{-0.0003613q^{-1} + 1.108q^{-2} + 2.333q^{-3} + 1.232q^{-4}}{1 + 2.062q^{-1} + 1.365q^{-2} + 0.24q^{-3} + 0.005785q^{-4}}, \quad (11)$$

where $k_m=0.7$, $LF=1.79574e^{-006}$, $FPE=1.94233e^{-006}$,

$$H(q) = \frac{0.001387q^{-1} + 0.8723q^{-2} + 1.817q^{-3} + 1.01q^{-4}}{1 + 1.39q^{-1} + 0.8062q^{-2} + 0.4463q^{-3} + 0.05838q^{-4}}, \quad (12)$$

where $k_m=0.95$, $LF=8.39577e^{-006}$, $FPE=9.03851e^{-006}$,

$$H(q) = \frac{0.0007292q^{-1} + 0.1354q^{-2} + 0.3375q^{-3} + 0.2565q^{-4}}{1 + 0.7763q^{-1} - 0.7749q^{-2} - 0.4494q^{-3} + 0.1483q^{-4}}, \quad (13)$$

where $k_m=0.99$, $LF=2.10871e^{-006}$, $FPE=2.25351e^{-006}$.

Below are the normalized transfer functions of OIM the type of *arx321* [15], magnetic coupling coefficients, self-generation frequencies, and deviation criteria for the self-generation mode:

$$H(q) = \frac{0.002866q^{-1} + 0.01125q^{-2}}{1 - 0.9517q^{-1} + 0.005012q^{-2} - 0.03896q^{-3}}, \quad (14)$$

where $k_m=0.7$, $f_{ag}=0.188$ Гц, $LF=0.000296686$, $FPE=0.000302316$,

$$H(q) = \frac{0.04551q^{-1} + 0.0439q^{-2}}{1 - 0.8355q^{-1} + 0.4682q^{-2} - 0.5434q^{-3}}, \quad (15)$$

where $k_m=0.95$, $f_{ag}=0.458$ Гц, $LF=0.000410605$, $FPE=0.000418166$,

$$H(q) = \frac{-0.004908q^{-1} + 0.1692q^{-2}}{1 - 0.4946q^{-1} - 0.2726q^{-2} - 0.06808q^{-3}}, \quad (16)$$

where $k_m=0.98$, $f_{ag}=0.721$ Гц, $LF=7.22731e^{-005}$, $FPE=7.36041e^{-005}$,

$$H(q) = \frac{0.1046q^{-1} + 0.2441q^{-2}}{1 - 0.2305q^{-1} - 0.6199q^{-2} + 0.1992q^{-3}}, \quad (17)$$

where $k_m=0.99$, $f_{ag}=1.017$ Гц, $LF=8.48779e^{-006}$, $FPE=8.65421e^{-006}$.

The above transfer functions of OIM correspond to the static transmission coefficients of the structural model of CRC $k_{UI}=\Delta I_q/\Delta U_s^*$: for (11) – $k_{UI}=0.2037$, (12) – $k_{UI}=1.5$, (13) – $k_{UI}=25.5$, (14) – $k_{UI}=18.4$, (15) – $k_{UI}=24.4$, (16) – $k_{UI}=26.2$, (17) – $k_{UI}=25.5$.

6. Discussion of results of studying of the charging resonance converter

Static characteristics of the structural model of CRC in Fig. 11–13 were obtained by averaging the values of transients in the parts where the processes were established. Transmission characteristics for power $I_q(U_s)$ in Fig. 11 are close to linear at $U_s > U_q$. In this supply voltage range, the primary and secondary circuits operate under resonant modes when the oscillation frequency is close to the resonant frequency of the circuit. The shape of the voltage at the input of the rectifier u_b is close to rectangular. Fluctuations in the circuit currents under the stationary mode have a constant amplitude. The linearity of the transmission characteristics was observed under the modes with forced generation and under the self-generation mode (dashed lines in Fig. 11), so it can be assumed that the CRC DM for the input on the supply voltage is also linear.

At $U_s < U_q$, the amplitude of oscillations on the magnetization inductance L_m is not sufficient to establish the resonance mode in the second circuit since the rectifier diodes do not open at all or open for a relatively small part of each semi-period of voltage. Oscillation mode depends on the ratio of the inductances of the scattering L_s and the magnetization inductance L_m , which is common to both contours. In such a two-circuit system, the resonance conditions are distributed between the serial resonance only with the scattering inductors and the mixed series-parallel resonance, in which the magnetization inductance is also involved [11, 18]. Therefore, at $U_s > U_q$, there is no constant ratio between the conditions of both types of resonance and the transfer characteristic of CRC is nonlinear, and the output current is too small (less than 5 % of the rated).

The dependences of the output current on the magnetic coupling coefficient $I_q(k_m)$ in Fig. 12 are significantly nonlinear. The greatest nonlinearity of the characteristics is observed under the mode with forced generation (curves A). When the magnetic connection between the coils k_m decreases, the scattering inductances L_s , which determine the frequencies of successive resonances, increase sharply. Since the operating frequency does not change, the resistances of the series RLC circuits increase and the amplitude of oscillations, as well as the output current, decrease quite quickly. However, under a self-generation mode, with the same changes in the magnetic coefficient, the output current changes to a lesser extent. The dependence of the output current on the magnetic coupling coefficient decreases with an increase in the time constant time of PhSF τ_{pf} since the self-generation frequency approaches the resonant frequency. This can be seen from the comparison of the characteristics A, B, and C.

The dependences of the self-generation frequency on the magnetic coupling coefficient in Fig. 13 for two values of the time constant of PhSF τ_{pf} are similar to each other. These dependences can be used to determine the sensitivity coefficient of the system over the perturbation channel as $k_{sm} = \Delta F_g / \Delta k_m$ under the CRC operating mode.

Fig. 14 shows the plots of the processes of the *Simulink* model of CRC for the magnetic coupling coefficient $k_m = 0.7$ and the modes of forced generation and self-generation. Plots in Fig. 14 were compared with the oscillograms of the circuit model of CRC and with the signals of experimental laboratory samples of resonant converters. Convergence of modeling plots in Fig. 14 with oscillograms additionally indicates that the structural model corresponds to the real scheme of CRC.

Transient characteristics for a constant operating frequency under the mode with forced generation in Fig. 15, a–c have an oscillatory character when the operating frequency is removed from the resonant one. This is explained by the fact that in the double-circuit oscillatory system of CRC, the phenomena of beats are observed. Along with forced oscillations at the operating frequency (they can appear in pulsations of the rectified current), there are two types of oscillations. The first type is oscillations with a difference between the operating frequency and the resonant frequency of the primary or secondary circuit. Oscillations of the second type are oscillations with a frequency equal to the difference in the resonance frequencies of the circuits, which, when interacting, modulate oscillations of the first type. As k_m increases, the resonant frequencies of the circuits approach the operating frequency and the oscillatory pattern of CRC decreases. Transient processes for envelope oscillations become aperiodic.

Transitional characteristics for the mode with self-generation in Fig. 14, d–j at different k_m are predominantly aperiodic in nature since the operating frequency remains close to the frequency of successive resonances. The phenomena of beats are not observed. They are characterized by rapid attenuation and long periods of oscillation.

The transitional characteristics of the structural models of CRC (curves 1 in Fig. 14) are combined with the transitional characteristics of OIM (curves 2 in Fig. 14). In some areas, the characteristics are quite close and, therefore, the plots visually coincide. For a regime with forced generation, the best convergence was provided by discrete-continuous OIM of the 4th order (see the value of the error criteria in (14) to (16)). With larger orders of OIM, approximation errors did not decrease significantly. For the self-generation mode, the processes are aperiodic in nature, so the best convergence of transients was provided by OIM of the 3rd order (the value of the error criteria in (17) to (20)).

The results of our research will be useful to engineers, scientists, and lecturers at technical universities in power electronics and conversion equipment, primarily in the design of charging systems with contactless transmission of electricity.

The conditions for applying the results of our work are the stage of preliminary formation of the structure of the power supply system or charging system and planning experiments in the process of design work. In further full-scale experiments, the results of research are refined.

Important limitations of the results of this work are switching processes in power keys. Switching processes, as a rule, are not taken into consideration in structural models intended for studying the «macro» dynamics of converters and can be investigated using mathematical models that combine switching processes and processes between switching moments. Also in this study, the system of inductively connected coils is considered linear but real inductors can interact with ferromagnetic media with nonlinear characteristics.

Potentially expected effects of the implementation of the results in design activities are the reduction of time for determining the dynamic characteristics and transfer functions of converters by computer modeling and algebraic analysis compared to typical procedures for identifying such converters by processing experimental data from a prototype.

Further advancement of the study is to take into consideration the nonlinearities of the system of inductors and the establishment of new patterns between the parameters of the elements of the converter circuits and the coefficients of its transfer functions.

7. Conclusions

1. A structural model of a charging resonance converter for non-contact transmission of electricity has been built, which makes it possible to investigate its dynamics and obtain equivalent transfer functions of a smaller order than transfer functions, which can be obtained by a purely analytical method.

2. Model experiments were carried out, as a result of which the dynamic characteristics of the resonant charger were determined. From practice, it turned out that the order of numerators and denominators of the obtained discrete transfer functions should be unity greater than the corresponding orders of equivalent continuous transfer functions.

3. A dynamic model was constructed by the method of system identification and the study into the dynamics of the con-

verter was carried out. A nonlinear DM of the converter for small signals in the first approximation can be represented as a set of nonlinear (possibly discrete) inertia-free part and linear inertial part. To determine the non-stationary DM, it would be advisable to take into consideration the variable switching period of the transducer when changing the total inductances of the coils and the magnetic coupling between them due to displacement.

Conflict of interest

The authors declare that they have no conflict of interest in relation to this research, whether financial, personal, authorship or otherwise, that could affect the research and its results presented in this paper.

References

1. Bose, B. K. (2013). *Modern Power Electronics and AC Drives*. PHI Learning Pvt Ltd.
2. Siroos, A., Sedighzadeh, M., Afjei, E., Fini, A. S., Yarkarami, S. (2021). Correction to: System Identification and Control Design of a Wireless Charging Transfer System with Double-Sided LCC Converter. *Arabian Journal for Science and Engineering*, 46 (10), 10287–10288. doi: <https://doi.org/10.1007/s13369-021-05726-0>
3. Pavlov, G., Obrubov, A., Vynnychenko, I. (2021). Design Procedure of Static Characteristics of the Resonant Converters. 2021 IEEE 3rd Ukraine Conference on Electrical and Computer Engineering (UKRCON). doi: <https://doi.org/10.1109/ukrcon53503.2021.9575698>
4. Pavlov, G., Pokrovskiy, M., Vinnichenko, I. (2018). Load Characteristics of the Serial-to-serial Resonant Converter with Pulse-number Regulation for Contactless Inductive Energy Transfer. 2018 IEEE 3rd International Conference on Intelligent Energy and Power Systems (IEPS). doi: <https://doi.org/10.1109/ieps.2018.8559590>
5. Pavlov, G., Obrubov, A., Vinnichenko, I. (2016). The linearized dynamic model of the series resonant converter for small signals. 2016 2nd International Conference on Intelligent Energy and Power Systems (IEPS). doi: <https://doi.org/10.1109/ieps.2016.7521879>
6. Tian, H., Tzelepis, D., Papadopoulos, P. N. (2021). Electric Vehicle Charger Static and Dynamic Modelling for Power System Studies. *Energies*, 14 (7), 1801. doi: <https://doi.org/10.3390/en14071801>
7. Tian, S., Lee, F. C., Li, Q., Li, B. (2015). Small-signal equivalent circuit model of series resonant converter. 2015 IEEE Energy Conversion Congress and Exposition (ECCE). doi: <https://doi.org/10.1109/ecce.2015.7309685>
8. Yin, Y., Zane, R., Erickson, R., Glaser, J. (2003). Direct modeling of envelope dynamics in resonant inverters. IEEE 34th Annual Conference on Power Electronics Specialist, 2003. PESC '03. doi: <https://doi.org/10.1109/pesc.2003.1216778>
9. Jain, A., Massimiani, I. C. (2021). LCC Resonant Converter Design and Transfer Function Computation Using FHA Analysis. 2021 4th Biennial International Conference on Nascent Technologies in Engineering (ICNTE). doi: <https://doi.org/10.1109/icnte51185.2021.9487672>
10. González-González, J., Triviño-Cabrera, A., Aguado, J. (2018). Design and Validation of a Control Algorithm for a SAE J2954-Compliant Wireless Charger to Guarantee the Operational Electrical Constraints. *Energies*, 11 (3), 604. doi: <https://doi.org/10.3390/en11030604>
11. Zheng, K., Zhang, G., Zhou, D., Li, J., Yin, S. (2018). Modeling, dynamic analysis and control design of full-bridge LLC resonant converters with sliding-mode and PI control scheme. *Journal of Power Electronics*, 18 (3), 766–777. doi: <https://doi.org/10.6113/JPE.2018.18.3.766>
12. Wang, W., Shi, Y., Yang, D. (2008). A New Modeling Method for the Switching Power Converter. 2008 Workshop on Power Electronics and Intelligent Transportation System. doi: <https://doi.org/10.1109/peits.2008.117>
13. Valdivia, V., Barrado, A., Lazaro, A., Fernandez, C., Zumel, P. (2010). Black-box modeling of DC-DC converters based on transient response analysis and parametric identification methods. 2010 Twenty-Fifth Annual IEEE Applied Power Electronics Conference and Exposition (APEC). doi: <https://doi.org/10.1109/apec.2010.5433361>
14. Valdivia, V., Barrado, A., Laazaro, A., Zumel, P., Raga, C., Fernandez, C. (2009). Simple Modeling and Identification Procedures for «Black-Box» Behavioral Modeling of Power Converters Based on Transient Response Analysis. *IEEE Transactions on Power Electronics*, 24 (12), 2776–2790. doi: <https://doi.org/10.1109/tpel.2009.2030957>
15. Gilat, A. (2014). *MATLAB: An Introduction with Applications*. Wiley. Available at: https://www.academia.edu/20361006/MATLAB_5th_Edition
16. Dongming, G., Dangshu, W. (2021). Research on Transmission Characteristics of Dual LCL Resonance Compensation Topology in Wireless Charging System. 2021 IEEE 5th Information Technology, Networking, Electronic and Automation Control Conference (ITNEC). doi: <https://doi.org/10.1109/itnec52019.2021.9586815>
17. Pentegov, I. V., Rymar, S. V., Volkov, I. V. (2006). Svyaz' mezhdru parametrami elektromagnitnykh, printsipial'nykh skhem i skhem zamesheniya dvukhobmotochnykh transformatorov. *Elektrotehnika i Elektromekhanika*, 3, 67–79. Available at: https://www.researchgate.net/publication/313140828_Svaz_mezdu_parametrami_elektromagnitnyh_principalnyh_shem_i_shem_zamesenia_dvuhobmotocnyh_transformatorov_Link_between_parameters_of_electromagnetic_principle_circuits_and_equivalent_circuits_of_doub
18. Wan, H. (2012). High Efficiency DC-DC Converter for EV Battery Charger Using Hybrid Resonant and PWM Technique. *Blackburg*, 115. Available at: https://vtechworks.lib.vt.edu/bitstream/handle/10919/32343/Wan_HM_T_2012.pdf